Protein-Protected Nanoparticles from Rapid Expansion of Supercritical Solution into Aqueous Solution

Mohammed J. Meziani,[†] Harry W. Rollins,[†,‡] Lawrence F. Allard,[§] and Ya-Ping Sun*[,†]

Department of Chemistry and Center for Advanced Engineering Fibers and Films, Howard L. Hunter Chemistry Laboratory, Clemson University, Clemson, South Carolina 29634-0973, and High-Temperature Materials Laboratory, Oak Ridge National Laboratory, Oak Ridge, Tennessee 37831-6062

Received: May 22, 2002; In Final Form: July 30, 2002

Nanocrystalline silver particles were prepared via a supercritical fluid processing technique RESOLV (Rapid Expansion of a Supercritical Solution into a Liquid SOLVent) coupled with chemical reduction. The preparation involved the rapid expansion of a supercritical ammonia solution of silver nitrate into an ambient solution that contained sodium borohydride or hydrazine as reducing agent and poly(*N*-vinyl-2-pyrrolidone) (PVP) or bovine serum albumin (BSA) protein as the protection agent for the resulting nanoparticle suspension. The nanoparticles were characterized using UV/vis absorption, X-ray powder diffraction, and transmission electron microscopy methods. The results show that the BSA protein-protected Ag nanoparticles are much larger than those obtained with PVP as protection agent under otherwise the same experimental conditions but still maintain relatively narrow size distributions. Mechanistic implications of the results are discussed.

Introduction

The application of supercritical fluid technology to the preparation and processing of nanomaterials has attached much recent attention.[1−11] For example, several groups have reported the use of reverse micelles in supercritical fluids for the synthesis of nanoscale metal, metal sulfide, and metal halide particles.[3−5,7,11] A supercritical fluid processing technique known as RESS (Rapid Expansion of Supercritical Solution) has been applied to the preparation of micron-sized and submicron-sized polymer and other particles.[12−17] In our laboratory, we have developed a similar supercritical fluid rapid expansion method called RESOLV (Rapid Expansion of a Supercritical Solution into a Liquid SOLVent) for producing semiconductor and metal nanoparticles.[1,8−11] The nanoparticles thus obtained are small (generally less than 10 nm), with relatively narrow size distributions. An important feature of the RESOLV method is that it requires no nanoscale templates (such as nanoscale cavities in micelles) for the formation of nanoparticles. The supercritical fluid rapid expansion itself provides the templating effect.[1] Thus, the method offers a "clean" way to produce nanoscale materials, amenable to the preparation of biocompatible nanoparticles and nanoparticles that are coated with biological species.

The development of biologically significant and/or biocompatible nanomaterials has been an active research area.[18−27] Among the most widely reported is the use of biological systems to assemble nanoscale materials.[19−24] For example, DNA has been used to organize nanoparticles into functional structures.[19,20] Specific antibody−antigen coupling has also been used to organize gold and silver nanoparticles into extended three-dimensional networks.[21] An important step in these bio-assisted assemblies and organizations is to make the nanoscale materials biocompatible. Similarly, biocompatibility is essential to the potential application of luminescent nanocrystals in bio-imaging and bio-tagging.[25−27] For zinc sulfide (ZnS)-capped cadmium selenide (CdSe) nanocrystals, as an example, the biocompatibility was achieved by coupling the nanocrystals to biomolecules such as protein.[26] Separately, bovine serum albumin (BSA) protein has been used to form bioconjugates with luminescent cadmium telluride (CdTe) nanoparticles that are capped with L-cysteine.[27] Upon the conjugation with BSA, the CdTe nanoparticles exhibit significantly increased luminescence intensities. The luminescence enhancement has been attributed to the resonance energy transfer from the tryptophan moieties in BSA to CdTe nanoparticles acting as receptors for the protein antennae.[27]

Here we report the preparation of silver (Ag) nanoparticles via RESOLV coupled with chemical reduction. The nanoparticles were capped with BSA by using the protein as protection agent in the receiving aqueous solution in RESOLV. In addition to the biocompatibility, the BSA protein-protected Ag nanoparticles were found to be significantly larger than those obtained with poly(*N*-vinyl-2-pyrrolidone) (PVP) as protection agent. Mechanistic implications of the results are discussed.

Experimental Section

Materials. Silver nitrate ($AgNO_3$), hydrazine (N_2H_4), and sodium borohydride ($NaBH_4$) were obtained from Aldrich. PVP polymer samples of average molecular weights M_W of ∼55 000 and ∼360 000 and BSA protein were purchased from Sigma. Anhydrous ammonia (>99.99%) was supplied by Air Products. Ethanol, obtained from Fisher Scientific, was distilled over molecular sieves and then filtered before use. Water was deionized and purified by being passed through a Labconco WaterPros water purification system.

Measurements. UV/vis absorption spectra were measured on a computer-controlled Shimadzu UV-3100 spectrophotometer. Powder X-ray diffraction measurements were carried out

[†] Clemson University.
[‡] Present address: Chemistry Department, Idaho National Engineering and Environmental Laboratory, Idaho Falls, ID 83415-2208.
[§] Oak Ridge National Laboratory.

10.1021/jp0212747 CCC: $22.00
Published on Web 10/08/2002

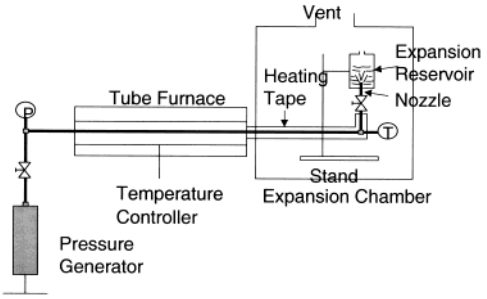

Figure 1. Experimental setup for RESOLV.

on a Scintag XDS-2000 powder diffraction system. Transmission electron microscopy (TEM) images were obtained on Hitachi 7000 and Hitachi HF-2000 TEM systems.

Gel electrophoresis analyses were carried out using the polyacrylamide gel of 12.5% concentration. In a typical experiment, the sample solution was mixed in a 1:1 ratio with a buffer containing Tris−HCl (250 mM, pH 6.8), glycerol (30%), and bromophenol blue (0.005%). An aliquot (10 fL) of the mixture was injected into the gel wells. The analysis was conducted in a Tris−glycine buffer for nondenaturing native protein gels at room temperature (running time 50 min at 300 V).

Nanoparticles. The apparatus for RESOLV is illustrated in Figure 1. In a typical experiment, a methanol solution of $AgNO_3$ (0.15 M, 0.5 mL) was added to a syringe pump, followed by the evaporation of the solvent methanol. The syringe pump was loaded with liquid ammonia (60 mL), and the mixture was then heated and equilibrated at 160 °C. The supercritical ammonia solution of $AgNO_3$ was rapidly expanded via a fused silica capillary nozzle (50 μm inner diameter) into a room-temperature solution of $NaBH_4$ (10 mg/mL) or N_2H_4 (80 mg/mL) in ethanol or water. The system pressure was maintained at 4000 psia during the rapid expansion. The receiving ethanol or water solution also contained PVP (5 mg/mL) or BSA (5 mg/mL) as protection agent to stabilize the Ag nanoparticle suspension.

Results and Discussion

PVP-Protected Nanoparticles. Nanocrystalline Ag particles were produced by rapidly expanding a supercritical ammonia solution of $AgNO_3$ into a room-temperature (22 °C) ethanol solution of $NaBH_4$ and PVP. The resulting PVP-protected nanoparticles formed a stable suspension indistinguishable from a typical colored homogeneous solution. The UV/vis absorption spectrum of the nanoparticle suspension is shown in Figure 2. The spectrum exhibits the characteristic surface plasmon absorption band of nanoscale Ag particles at ~400 nm. A typical TEM image of the nanoparticles on a collodion film-coated copper grid is shown in Figure 3. From the TEM result, a statistical analysis of 200 particles yields an average Ag nanoparticle size of 4.8 nm in diameter and a size distribution standard deviation of 0.8 nm (Table 1).

Aqueous receiving solution was also used with the RESOLV process. As compared in Figure 2, the surface plasmon absorption band of the Ag nanoparticles in aqueous suspension peaks at a similar wavelength but is of a narrower bandwidth than that of the nanoparticles in an ethanol suspension. The Ag nanoparticles obtained via RESOLV with aqueous receiving solution are on-average larger, with a broader size distribution (Figure 3, Table 1). According to Henglein, PVP is a less effective protection agent for colloid Ag particles in water than in ethanol.[28] Thus, the larger Ag nanoparticles obtained with aqueous receiving solution are probably a result of relatively more efficient particle growth due to the less effective protection

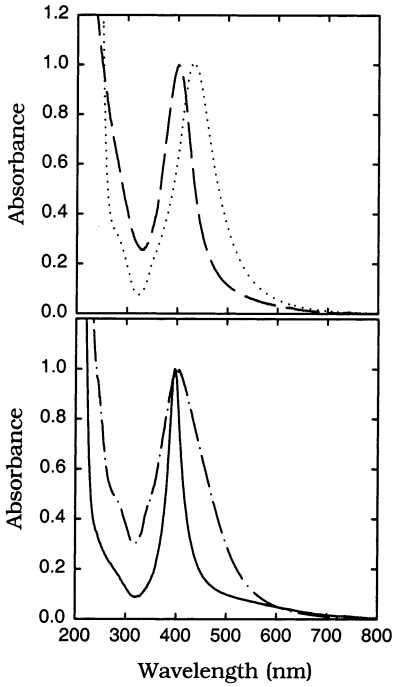

Figure 2. UV/vis absorption spectra of the Ag nanoparticles prepared via RESOLV with $NaBH_4$ and PVP in ethanol (− − −), hydrazine and PVP in ethanol (···), $NaBH_4$ and PVP in water (—), and $NaBH_4$ and BSA in water (−·−).

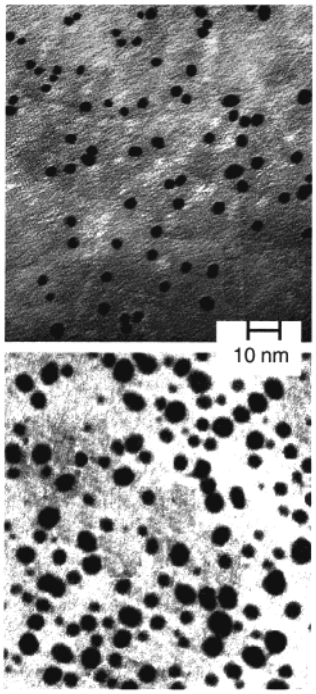

Figure 3. TEM images of the Ag nanoparticles prepared via RESOLV with $NaBH_4$ reduction and PVP as protection agent in ethanol (top) and aqueous (bottom) receiving solutions.

of PVP in aqueous medium. The results also suggest that the protection agent may play a significant role in the nanoparticle formation in RESOLV with chemical reduction.

The formation of Ag nanoparticles is also dependent on the reducing agent. When hydrazine was used for reduction in the receiving ethanol solution, the Ag nanoparticles were larger than those obtained in reduction with $NaBH_4$ (Figure 4, Table 1).[10] The surface plasmon absorption band of the Ag nanoparticles obtained from the hydrazine reduction is broader and red-shifted

TABLE 1: Parameters of Ag Nanoparticles Produced via RESOLV with Chemical Reduction

receiving solution	protection agent[a]	reducing agent	average particle size (nm) TEM[b]	X-ray
ethanol	PVP	$NaBH_4$	4.8 (0.8)	6
aqueous	PVP	$NaBH_4$	6.1 (1.6)	
aqueous	PVP [c]	$NaBH_4$	6.9 (2.0)	
ethanol	PVP	hydrazine	6.2 (1.8)	
aqueous	BSA	$NaBH_4$	27 (6.8)	21
aqueous	BSA	hydrazine	43 (10)	

[a] Unless specified otherwise, the molecular weight of PVP is 360 000. [b] The value in parentheses is the size distribution standard deviation. [c] Molecular weight of 55 000.

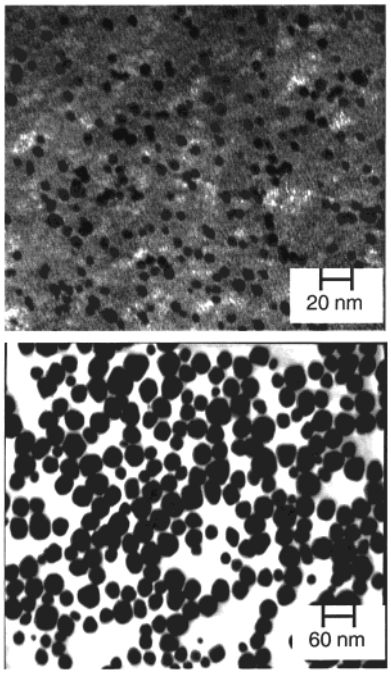

Figure 4. TEM images of the Ag nanoparticles prepared via RESOLV with hydrazine reduction and with PVP in ethanol receiving solution (top) and BSA in aqueous receiving solution (bottom).

(Figure 2). The absorption spectral changes might be attributed to a combination of effects, including a larger average particle size and perhaps different nanoparticle surface properties due to the presence of hydrazine and related nitrogen-containing species (from the reduction) on the nanoparticle surface.

The nanocrystalline Ag particles were identified in X-ray powder diffraction analyses. For the Ag nanoparticle sample prepared via RESOLV with PVP as protection agent in ethanol receiving solution, a typical X-ray powder diffraction pattern is shown in Figure 5, which matches well with the pattern for Ag (fcc) in the JCPDS reference library. The average particle size estimated from the Debeye−Scherer equation[29] is 6 nm, which is comparable with the result obtained from the statistical analysis of the TEM images. This supports the notion that the Ag nanoparticles are highly crystalline with the crystal grain sizes (detectable by X-ray powder diffraction) being similar to the particle sizes (measurable by TEM imaging).

BSA-Protected Nanoparticles. BSA protein was used to replace PVP as protection agent in the receiving aqueous solution for RESOLV, allowing the preparation of BSA-protected Ag nanoparticles without the need to introduce potentially unwanted materials or impurities. These nanoparticles exhibit some different properties from those of the PVP-protected nanoparticles.

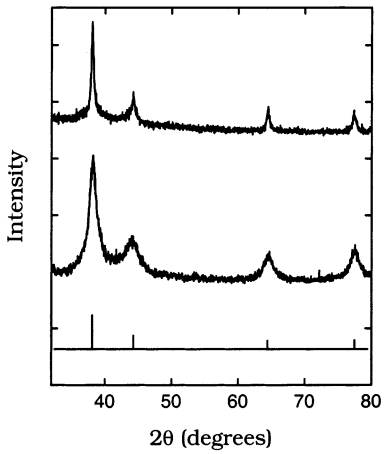

Figure 5. X-ray powder diffraction patterns of the Ag nanoparticles prepared via RESOLV with $NaBH_4$ reduction and with BSA in aqueous receiving solution (top) and PVP in ethanol receiving solution (bottom). The Ag pattern from the JCPDS database is also shown for comparison.

For Ag nanoparticles produced in RESOLV, BSA is a protection agent as effective as PVP. The BSA-protected Ag nanoparticles also form a stable aqueous suspension that resembles a homogeneous solution. The UV/vis absorption spectrum of the suspension is compared in Figure 2 with those of the PVP-protected Ag nanoparticles. The surface plasmon absorption band of the BSA-protected Ag nanoparticles is broader and slightly red-shifted, probably reflecting more of changes in the nanoparticle surface properties due to interactions with the protein species. Surprisingly, however, results from the TEM imaging show that the BSA-protected Ag nanoparticles are substantially larger in size than the PVP-protected Ag nanoparticles and that the size distributions remain relatively narrow (Table 1). For example, the BSA-protected Ag nanoparticles obtained with the hydrazine reduction (Figure 4) have an average particle size almost 7 times that of the PVP-protected Ag nanoparticles obtained under otherwise the same experimental conditions (Table 1).

The solid-state samples of the BSA-protected Ag nanoparticles were also characterized by X-ray powder diffraction analyses. The diffraction patterns again match well with that of Ag (fcc) in the JCPDS reference library (Figure 5). The diffraction peaks of these samples are generally less broad than those of the PVP-protected Ag nanoparticle samples, consistent with fact that the Ag nanoparticles in these samples are larger. The average Ag nanoparticle sizes estimated in terms of eq 1 are comparable with those obtained from the TEM images (Table 1).

The BSA protein contains 60 amino moieties in lysine residues, 26 arginine moieties in guanidino side chains, and many thiol groups,[30] which may be attractive to the Ag nanoparticle surface. It was a concern that small Ag nanoparticles might attach to the protein to form dendrimer-like three-dimensional structures, which could appear as larger nanoparticles in the TEM imaging. The X-ray powder diffraction results of the BSA-protected Ag nanoparticles suggest large Ag crystal grains, which are inconsistent with any BSA protein-supported dendritic assemblies of smaller Ag nanoparticles. However, one might still argue that the X-ray results correspond to solid-state samples of the nanoparticles, which could be different from the species in a stable suspension. The suspended species are better represented by the samples on copper grids for TEM analyses. Thus, the TEM samples were imaged at high resolution to examine the crystal lattice fringes in individual Ag nanoparticles. Shown in Figure 6 is a comparison of high-resolution TEM

SCHEME 1

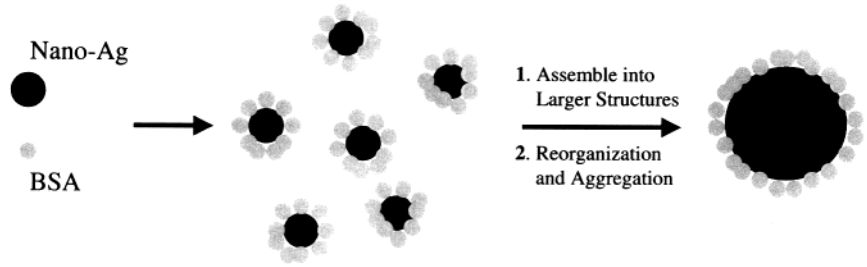

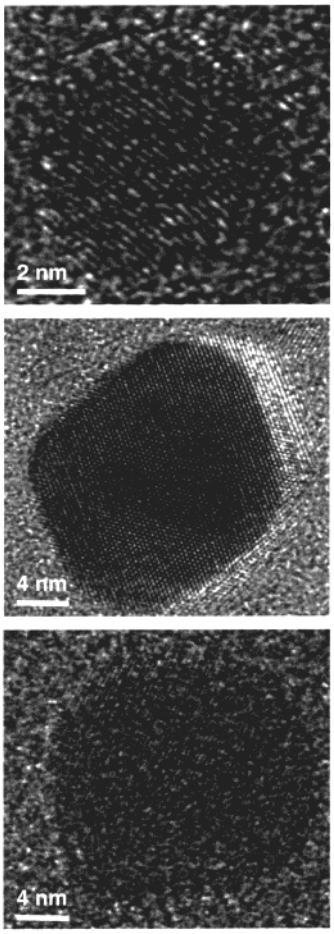

Figure 6. High-resolution TEM images of three Ag nanoparticles prepared via RESOLV with $NaBH_4$ reduction and with PVP in ethanol receiving solution (top) and BSA in aqueous receiving solution (middle and bottom).

images of several Ag nanoparticles. The lattice fringes in all these images generally have a spacing of 0.24 nm, corresponding to the (111) plane for Ag. The PVP-protected Ag nanoparticle in Figure 6a appears to be a single crystal, which represents the majority of the Ag nanoparticles thus produced via RESOLV. The much larger BSA-protected Ag nanoparticles (Figure 6b,c) are polycrystalline with multiple misaligned lattice fringes. The results seem to suggest that the BSA-protected Ag nanoparticles are probably agglomerated smaller nanoparticles. However, there is no evidence for any protein-supported dendritic assemblies of small Ag nanoparticles.

The formation of larger Ag nanoparticles in RESOLV with BSA as protection agent is not due to the relatively low molecular weight of the BSA protein (66 431). In a control experiment, PVP with molecular weight M_W of 55 000 was used in RESOLV. The Ag nanoparticles thus prepared were similar to those obtained with high molecular weight PVP (M_W = 360 000) as protection agent (Table 1). The nanoparticle size was insensitive to the concentration of PVP[31] or BSA. For example, doubling the BSA concentration resulted in only marginal changes in the size of the nanoparticles.

The BSA-protected Ag nanoparticles were analyzed by gel electrophoresis. The results show that the two bands corresponding to BSA monomer and dimer are much weaker in the nanoparticle sample than in the blank BSA sample and that the majority of the nanoparticle sample becomes stationary, appearing at the gel onset. It is logical to assign these species of low mobility to BSA-protected Ag nanoparticles.[32] An investigation on the biocompatibility of the BSA-protected nanoparticles is in progress.

It is somewhat surprising that the Ag nanoparticles produced in the same RESOLV process but with different protection agents (PVP vs BSA) are of dramatically different average sizes. The results suggest that the protection agent in the receiving solution plays an important role in the nanoparticle formation and growth in the RESOLV process. However, the role of BSA as protection agent is probably special, because the use of other polymeric protection agents in RESOLV has yielded nanoparticles that are comparable with those produced with PVP as protection agent.[31,33] Also interesting is the fact that the much larger BSA-protected Ag nanoparticles maintain relatively narrow size distributions, suggesting that these larger nanoparticles are not from smaller nanoparticles via a simple agglomeration process. Instead, there might be a more specific process for the assembly of the smaller Ag nanoparticles produced initially in RESOLV with chemical reduction, and the resulting assemblies serve as intermediates in the agglomeration to form the larger Ag nanoparticles. As illustrated in Scheme 1, one possibility is that the initially formed nanoparticle−BSA conjugates assemble, which might be driven by the protein aggregation, to form larger but relatively well-organized structures. The agglomeration of the Ag nanoparticles in these structures, which might be facilitated by the reorganization of the assemblies, results in the formation of the larger BSA-protected Ag nanoparticles.

Apparently, a more definite understanding of the role of BSA in the formation of larger Ag nanoparticles in RESOLV with chemical reduction requires further investigations. Nevertheless, the available results have demonstrated the potential to alter the properties of the nanoparticles produced via RESOLV by varying the experimental conditions.

Acknowledgment. We thank Yi Lin, Daniel Zweifel, and Darron Hill for experimental assistance. Financial support from DOE (DE-FG02-00ER45859) and the Center for Advanced Engineering Fibers and Films (NSF-ERC at Clemson University) is gratefully acknowledged. We also acknowledge the sponsorship by the Assistant Secretary for Energy Efficiency and Renewable Energy, Office of Transportation Technologies,

as part of the HTML User Program, ORNL, managed by UT-Battelle, LLC, for DOE (DE-AC05-00OR22725).

References and Notes

(1) Sun, Y.-P.; Rollins, H. W.; Jayasundera, B.; Meziani, M. J.; Bunker, C. E. In *Supercritical Fluid Technology in Materials Science and Engineering: Synthesis, Properties, and Applications*; Sun, Y.-P., Ed.; Marcel Dekker: New York, 2002; p 491.

(2) (a) Watkins, J. J.; McCarthy, T. J. *Chem. Mater*. **1995**, *7*, 1991. (b) Blackburn, J. M.; Long, D. P.; Cabanas, A.; Watkins, J. J. *Science* **2001**, *294*, 141.

(3) (a) Ji, M.; Chen, X. Y.; Wai, C. M.; Fulton, J. L. *J. Am. Chem. Soc*. **1999**, *121*, 2631. (b) Ohde, H.; Rodriguez, J. M.; Ye, X. R.; Wai, C. M. *Chem. Commun*. **2000**, *23*, 2353.

(4) Ohde, H.; Hunt, F.; Wai, C. M. *Chem. Mater*. **2001**, *13*, 4130.

(5) (a) Holmes, J. D.; Bhargava, P. A.; Korgel, B. A.; Johnston, K. P. *Langmuir* **1999**, *15*, 6613. (b) Shah, P. S.; Holmes, J. D.; Doty, R. C.; Johnston, K. P.; Korgel, B. A. *J. Am. Chem. Soc*. **2000**, *122*, 4245.

(6) (a) Shah, P. S.; Husain, S.; Johnston, K. P.; Korgel, B. A. *J. Phys. Chem. B* **2001**, *105*, 9433. (b) Holmes, J. D.; Ziegler, K. J.; Doty, R. C.; Pell, L. E.; Johnston, K. P.; Korgel, B. A. *J. Am. Chem. Soc*. **2001**, *123*, 3743. (c) Ziegler, K. J.; Doty, R. C.; Johnston, K. P.; Korgel, B. A. *J. Am. Chem. Soc*. **2001**, *123*, 7797.

(7) (a) Cason, J. P.; Roberts, C. B. *J. Phys. Chem. B* **2000**, *104*, 1217. (b) Cason, J. P.; Khambaswadkar, K.; Roberts, C. B. *Ind. Eng. Chem. Res*. **2000**, *39*, 4749.

(8) (a) Sun, Y.-P.; Rollins, H. W. *Chem. Phys. Lett.* **1998**, *288*, 585. (b) Sun, Y.-P.; Guduru, R.; Lin, F.; Whiteside, T. *Ind. Eng. Chem. Res.* **2000**, *39*, 4663.

(9) Sun, Y.-P.; Rollins, H. W.; Guduru, R. *Chem. Mater*. **1999**, *11*, 7.

(10) Sun, Y.-P.; Riggs, J. E.; Rollins, H. W.; Guduru, R. *J. Phys. Chem. B* **1999**, *103*, 77.

(11) Sun, Y.-P.; Atorngitjawat, P.; Meziani, M. J. *Langmuir* **2001**, *17*, 5707.

(12) (a) Petersen, R. C.; Matson, D. W.; Smith, R. D. *J. Am. Chem. Soc.* **1986**, *108*, 2100. (b) Matson, D. W.; Norton, K. A.; Smith, R. D. *Chemtech* **1989**, *19*, 480.

(13) Eckert, C. A.; Knutson, B. L.; Debenedetti, P. G. *Nature* **1996**, *383*, 313.

(14) Tom, J. W.; Debenedetti, P. G. *J. Aerosol Sci.* **1991**, *22*, 555.

(15) Mawson, S.; Johnston, K. P.; Combes, J. R.; Desimone, J. M. *Macromolecules* **1995**, *28*, 3182.

(16) Lele, A. K.; Shine, A. D. *Ind. Eng. Chem. Res.* **1994**, *33*, 1476.

(17) Weber, M.; Thies, M. C. In *Supercritical Fluid Technology in Materials Science and Engineering: Synthesis, Properties, and Applications*; Sun, Y.-P., Ed.; Marcel Dekker: New York, 2002; p 387.

(18) Storhoff, J. J.; Mirkin, C. A. *Chem. Rev*. **1999**, *99*, 1849.

(19) (a) Mirkin, C. A.; Letsinger, R. L.; Mucic, R. C.; Storhoff, J. J. *Nature* **1996**, *382*, 607. (b) Elghanian, R.; Storhoff, J. J.; Mucic, R. C.; Letsinger, R. L.; Mirkin, C. A. *Science* **1997**, *277*, 1078.

(20) (a) Coffer, J. L.; Bigham, S. R.; Li, X.; Pinizzotto, R. F.; Rho, Y. G.; Pirtle, R. M.; Pirtle, I. L. *Appl. Phys. Lett.* **1996**, *69*, 3851. (b) Patel, A. A.; Wu, F. X.; Zhang, J. Z.; Torres-Martinez, C. L.; Mehra, R. K.; Yang, Y.; Risbud, S. H. *J. Phys. Chem. B* **2000**, *104*, 11598.

(21) Shenton, W.; Davis, S. A.; Mann, S. *Adv. Mater*. **1999**, *11*, 449.

(22) (a) Li, M.; Wong, K. K. W.; Mann, S. *Chem. Mater*. **1999**, *11*, 23. (b) Connolly, S.; Fitzmaurice, D. *Adv. Mater*. **1999**, *11*, 1202.

(23) Alivisatos, A. P.; Johnsson, K. P.; Peng, X. G.; Wilson, T. E.; Loweth, C. J.; Bruchez, M. P.; Schultz, P. G. *Nature* **1996**, *382*, 609.

(24) (a) Shi, J. F.; Bergstrom, D. E. *Angew. Chem., Int. Ed. Engl.* **1997**, *36*, 111. (b) Niemeyer, C. M. *Angew. Chem., Int. Ed. Engl.* **1997**, *36*, 585. (c) Whaley, S. R.; English, D. S.; Hu, E. L.; Barbara, P. F.; Belcher, A. M. *Nature* **2000**, *405*, 665.

(25) Bruchez, M.; Moronne, M.; Gin, P.; Weiss, S.; Alivisatos, A. P. *Science* **1998**, *281*, 2013.

(26) Chan, W. C. W.; Nie, S. *Science* **1998**, *281*, 2016.

(27) Mamedova, N. N.; Kotov, N. A.; Rogach, A. L.; Studer, J. *Nano Lett.* **2001**, *1*, 281.

(28) Henglein, A. *Chem. Mater*. **1998**, *10*, 444.

(29) Klug, H. P.; Alexander, L. E. *X-ray Diffraction Procedures*; John Wiley & Sons: New York, 1959.

(30) (a) Foster, J. F. In *Albumin Structure, Function and Uses*; Rosenoer, V. M., Oratz, M., Rothschild, M. A., Eds.; Pergamon: Oxford, U.K., 1977; p 53. (b) Hirayama, K., Akashi, S., Furuya, M., Fukuhara, K. I. *Biochem. Biophys. Res. Commun.* **1990**, *173*, 639. (c) Reed, R. G.; Putnam, F. W.; Peters, T., Jr. *Biochem. J.* **1980**, *191*, 867.

(31) Rollins, H. W. Ph.D. Dissertation, Clemson University, 1999.

(32) In a control experiment, BSA was subjected to the RESOLV conditions in the absence of $AgNO_3$. Except for minor denaturing (due primarily to the basicity of ammonia),[30] gel electrophoresis results of the treated BSA sample are similar to those of the blank BSA sample.

(33) Meziani, M. J.; Sun, Y.-P. Unpublished results.